

Effects of particle-number conservation on heat capacity of nuclei

K. Esashika

*Graduate School of Science and Technology,
Chiba University, Inage, Chiba 263-8522, Japan*

H. Nakada*

*Department of Physics, Faculty of Science,
Chiba University, Inage, Chiba 263-8522, Japan*

K. Tanabe[†]

*Department of Physics, Faculty of Science,
Saitama University, Sakura, Saitama 338-8570, Japan*

(Dated: August 10, 2018)

Abstract

By applying the particle-number projection to the finite-temperature BCS theory, the S -shaped heat capacity, which has recently been claimed to be a fingerprint of the superfluid-to-normal phase transition in nuclei, is reexamined. It is found that the particle-number (or number-parity) projection gives S -shapes in the heat capacity of nuclei which look qualitatively similar to the observed ones. These S -shapes are accounted for as effects of the particle-number conservation on the quasiparticle excitations, and occur even when we keep the superfluidity at all temperatures by assuming a constant gap in the BCS theory. The present study illustrates significance of the conservation laws in studying phase transitions of finite systems.

PACS numbers: 21.90.+f, 21.60.-n, 05.70.-a

While phase transitions are striking phenomena in infinite systems, it has been difficult to establish them in finite systems such as atomic nuclei, because their signatures are often obscured by the quantum fluctuations [1]. Since most nuclei have the superfluidity in their ground states, *i.e.* at zero temperature, the superfluid-to-normal transition for increasing temperature has been discussed theoretically [2, 3, 4, 5]. Recently, high precision measurement of nuclear level densities has been implemented [6], in which the level densities are extracted from the γ -ray data with the help of the Brink-Axel hypothesis. Converting the microcanonical information to the canonical one, they have found that S -shapes appear in the graphs of the heat capacity C as a function of temperature T . It has been argued that the S -shapes are a fingerprint of the superfluid-to-normal phase transition, since such S -shapes occur if continuity is taken between heat capacity in the superfluid phase (described by the constant- T model) and that in the normal fluid phase (described by the backshifted Bethe formula). Based on this picture, they estimated critical temperature from their experimental data. Similar S -shapes come out in theoretical calculations including the quantum fluctuations [3, 5].

The superfluid and the normal-fluid phases in nuclei are defined within the mean-field picture; in the Bardeen-Cooper-Schrieffer (BCS) theory or in the Hartree-Fock-Bogoliubov theory. In studying the superfluid-to-normal transition, linkage to the mean-field picture should carefully be traced, even when the S -shapes are reproduced by calculations including a variety of quantum fluctuations. Breakdown of a certain symmetry is often associated with phase transitions. In respect to the superfluid-to-normal transition, the particle-number conservation is violated in the superfluid phase while preserved in the normal-fluid phase, within the mean-field theories. However, this is an approximate picture and the particle-number conservation is not violated in actual nuclei, restored via the quantum fluctuations. Since restoration of the symmetry sometimes plays an important role particularly in finite systems, it is desired to investigate how the number conservation affects the heat capacity of nuclei.

The so-called number-parity forms a subgroup isomorphic to S_2 of the $U(1)$ group accompanied by the particle-number. The number-parity projection in the finite-temperature BCS (FT-BCS) theory [7] was developed more than two decades ago [8]. The full number projection at finite temperature is much more complicated task. There is a fundamental difficulty in the variation-after-projection scheme, though an approximate solution has recently been suggested [9]. On the other hand, the number projection in the variation-before-projection (VBP) scheme was formulated in Refs. [9, 10, 11]. In this paper, we apply the particle-number projection as well as the number-parity projection in the FT-BCS theory, and qualitatively investigate effects of the particle-number conservation in the heat capacity of nuclei. By the VBP scheme, we view effects only of the projected statistics, without changing the excitation spectra given by the BCS Hamiltonian, as a step of tracing effects of various quantum fluctuations.

We mainly consider the $^{161,162}\text{Dy}$ nuclei. Let us assume the following model Hamiltonian,

$$\hat{H} = \hat{H}_p + \hat{H}_n, \quad \hat{H}_\tau = \sum_{k \in \tau} \varepsilon_k a_k^\dagger a_k - \frac{g_\tau}{4} \sum_{k, k' \in \tau} a_k^\dagger a_{\bar{k}}^\dagger a_{\bar{k}'} a_{k'} \quad (\tau = p, n), \quad (1)$$

where \bar{k} indicates the time-reversal of the single-particle (s.p.) state k . The s.p. state k and its energy ε_k are determined from the Nilsson model [12], by assuming the quadrupole deformation from the measured $E2$ strength [13]. We take $g_p = 22/A$ and $g_n = 27/A$ MeV [14]. For the model space, we first define the Fermi energy ε_F for each nucleus by the arithmetic average between the energy of the highest occupied Nilsson s.p. level and that of the lowest unoccupied level, without the residual interaction. We then include all the s.p. levels satisfying $|\varepsilon_k - \varepsilon_F| < 7$ MeV, for both protons and neutrons. The g_τ values are related to the model space; with the present choice we reproduce the pairing gaps of $\Delta_\tau \approx 12/\sqrt{A}$ MeV. Although the Hamiltonian in Eq. (1) is relatively simple, it will be sufficient for qualitative study of the pairing phase transition. Note that the critical temperature of the deformed-to-spherical shape phase transition is appreciably higher than that of the superfluid-to-normal transition, and that the s.p. levels hardly change at $T \lesssim 1$ MeV [4].

In the FT-BCS theory, we introduce the auxiliary Hamiltonian

$$\hat{H}' = \hat{H}'_p + \hat{H}'_n, \quad \hat{H}'_\tau = \hat{H}_\tau - \lambda_\tau \hat{N}_\tau \quad (\tau = p, n), \quad (2)$$

where λ_τ stands for the chemical potential and \hat{N}_τ the number operator, $\hat{N}_\tau = \sum_{k \in \tau} a_k^\dagger a_k$. The quasiparticle (q.p.) operators are obtained from the Bogoliubov transformation,

$$\alpha_k = u_k a_k - v_k a_{\bar{k}}^\dagger, \quad (3)$$

with $u_k^2 + v_k^2 = 1$, and the q.p. energy is given by

$$E_k = \sqrt{\tilde{\varepsilon}_k^2 + \Delta_\tau^2}; \quad \tilde{\varepsilon}_k = \varepsilon_k - g_\tau v_k^2 - \lambda_\tau, \quad \Delta_\tau = \frac{g_\tau}{2} \sum_{k \in \tau} u_k v_k. \quad (4)$$

The density operator in the FT-BCS theory is

$$\hat{w}_0 = \frac{e^{-\hat{H}_0/T}}{\text{Tr}(e^{-\hat{H}_0/T})}; \quad \hat{H}_0 = \sum_k E_k \alpha_k^\dagger \alpha_k. \quad (5)$$

Here Tr denotes the grand-canonical trace in the model space. The thermal expectation value of an observable \hat{O} is calculated by $\langle \hat{O} \rangle_0 = \text{Tr}(\hat{w}_0 \hat{O})$. Equation (5) is an approximation of \hat{H}' in the Boltzmann-Gibbs operator $e^{-\hat{H}'/T}$ by (const. + \hat{H}_0). The entropy is defined by $S = -\text{Tr}(\hat{w}_0 \ln \hat{w}_0)$. The FT-BCS equation, which determines the u_k and v_k coefficients in Eq. (3), is obtained so as to minimize the grand potential $\Omega = \langle \hat{H}' \rangle_0 - TS$ for each T [7]. The chemical potential λ_τ is fixed by the particle-number condition $\langle \hat{N}_\tau \rangle_0 = N_\tau$, where N_τ is the particle number in the model space corresponding to the specific nuclide.

Introducing the particle-number projector,

$$\hat{P}_\tau = \frac{1}{2\pi} \int_{-\pi}^{\pi} d\varphi e^{-i\varphi(\hat{N}_\tau - N_\tau)}, \quad (6)$$

we define the density operator in the projected statistics,

$$\hat{w}_P = \frac{\hat{P}_p \hat{P}_n e^{-\hat{H}_0/T} \hat{P}_p \hat{P}_n}{\text{Tr}(\hat{P}_p \hat{P}_n e^{-\hat{H}_0/T})}. \quad (7)$$

The thermal expectation value in the number-projected statistics is obtained by $\langle \hat{O} \rangle_P = \text{Tr}(\hat{w}_P \hat{O})$. The integration over φ in Eq. (6) takes account of a certain part of the two-body correlations beyond the mean-field approximation. In practical calculations, the φ integral is replaced by a discrete sum:

$$\hat{P}_\tau = \frac{1}{M+1} \sum_{m=0}^M e^{-i\varphi_m(\hat{N}_\tau - N_\tau)}, \quad (8)$$

where M stands for the number of the s.p. states and $\varphi_m = 2\pi m/(M+1)$. If we set $M=1$ instead of the number of the s.p. states in Eq. (8), \hat{P}_τ is reduced to the number-parity projector [9],

$$\hat{P}'_\tau = \frac{1}{2} \sum_{\varphi=0,\pi} e^{-i\varphi(\hat{N}_\tau - N_\tau)}. \quad (9)$$

Correspondingly, \hat{w}_P and $\langle \hat{O} \rangle_P$ become those of the number-parity projection, which we shall denote by $\hat{w}_{P'}$ and $\langle \hat{O} \rangle_{P'} = \text{Tr}(\hat{w}_{P'} \hat{O})$. In this paper we distinguish the unprojected, the number-projected and the number-parity-projected expectation values by the suffices as $\langle \hat{O} \rangle_0$, $\langle \hat{O} \rangle_P$ and $\langle \hat{O} \rangle_{P'}$, respectively.

We here calculate heat capacity by $C = d\langle \hat{H} \rangle / dT$, which is obtained by numerical differentiation of $\langle \hat{H} \rangle$ for various T , in practice. In Fig. 1, the heat capacities with and without projection (C_0 , $C_{P'}$ and C_P) are depicted for ^{162}Dy . There occur two discontinuities in $C(T)$, corresponding to the superfluid-to-normal transitions for protons and neutrons. This is confirmed by Δ_p and Δ_n , which rapidly vanish at the respective critical temperature T_c . This signature to the transition does not disappear by the projection because it is implemented after variation. Although such discontinuities are unrealistic, the present purpose is to investigate effects of the projection mainly at $T < T_c$. We have $T_c \approx 0.5 - 0.6$ MeV in the present calculation, slightly lower for protons than for neutrons. In the normal fluid phase, the projections do not make important differences; difference of the number-parity-projected result from the unprojected one is even almost invisible. At $T < T_c$, we find that there is a certain effect of the projection on $C(T)$, either the number-parity or the number projection; an *S*-shape appears when we apply the number or the number-parity projection. It is noted that, in the number-parity projection, the zero-point of the energy may influence $C_{P'}$, since $\langle \hat{N}_\tau \rangle_{P'}$ is displaced from N_τ depending on T because of the incomplete projection (after variation). To suppress this influence, we use $(\varepsilon_k - \varepsilon_F)$ instead of ε_k in the Hamiltonian of Eq. (1).

Since the proton and neutron degrees-of-freedom are separated in the Hamiltonian of Eq. (1), we have $C = C_p + C_n$, where $C_\tau = d\langle \hat{H}_\tau \rangle / dT$. We present $C_n(T)$ for ^{162}Dy in

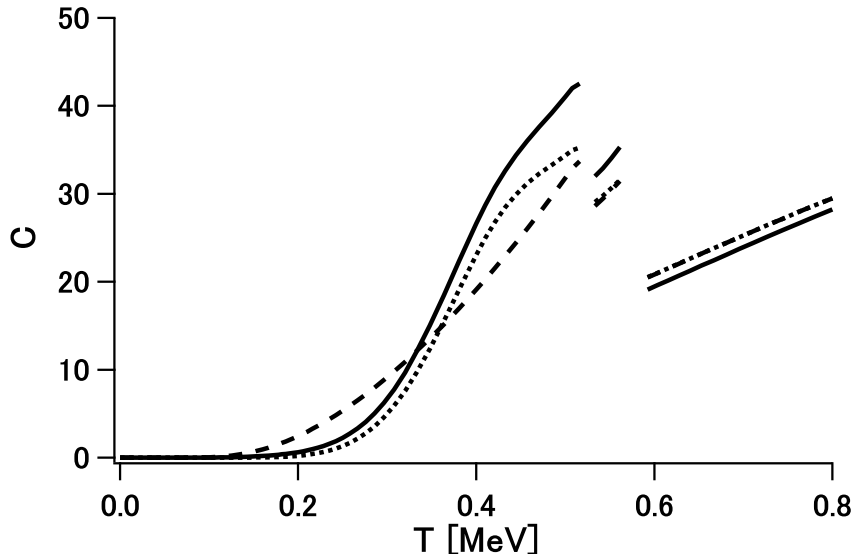


FIG. 1: Heat capacity C vs. temperature T for ^{162}Dy . The dashed line is obtained by the FT-BCS calculation without projection, while the solid and dotted lines are with the number and the number-parity projections, respectively.

Fig. 2(a), so as to simplify discussions. There is no qualitative difference between $C_p(T)$ and $C_n(T)$. It is noticed that, while $C_{n,0} = d\langle\hat{H}_n\rangle_0/dT$ increases almost linearly at $(0.2 \text{ MeV} \lesssim T < T_c)$, an S -shape comes out both in $C_{n,P'} = d\langle\hat{H}_n\rangle_{P'}/dT$ and $C_{n,P} = d\langle\hat{H}_n\rangle_P/dT$ in this temperature region. In order to view effects of the projections more clearly, we also show $\Delta E_{n,P} = \langle\hat{H}_n\rangle_P - \langle\hat{H}_n\rangle_0$ and $\Delta E_{n,P'} = \langle\hat{H}_n\rangle_{P'} - \langle\hat{H}_n\rangle_0$ as a function of T , in Fig. 2(b). Obviously, the slope in $\Delta E_{n,P}(T)$ is equal to the difference of $C_{n,P}$ from $C_{n,0}$, and likewise for $\Delta E_{n,P'}(T)$. In this respect, the S -shape in the number-parity-projected case comes from the decrease of $\Delta E_{n,P'}(T)$ at $0.2 \lesssim T \lesssim 0.35 \text{ MeV}$ as well as the increase at $0.35 \lesssim T \lesssim 0.5 \text{ MeV}$. This behavior does not change by the full particle-number projection, although $\Delta E_{n,P}(T)$ shifts downward to a certain extent, compared with $\Delta E_{n,P'}(T)$. We also plot in Fig. 2(c) the expectation value of the q.p. number $\langle\hat{\mathcal{N}}_n\rangle$, where $\hat{\mathcal{N}}_n = \sum_{k \in n} \alpha_k^\dagger \alpha_k$. In Fig. 2(c), the number-parity-projected result is almost indistinguishable from the fully number-projected result at $T \lesssim 0.5 \text{ MeV}$, and from the unprojected one at $T \gtrsim 0.5 \text{ MeV}$. At $T \approx 0$, we have $\langle\hat{\mathcal{N}}_n\rangle \approx 0$ as it should be. As T goes up slightly to about 0.2 MeV , excitation to the 1 q.p. states gives rise to increase of $\langle\hat{H}\rangle_0$, and yields dominant contribution to $C_{n,0}$. However, this is fictitious, resulting from the violation of the number or the number-parity conservation. Since the 1 q.p. states are removed, $\langle\hat{H}\rangle_{P'}$ tends to stay at its $T = 0$ value, giving the decrease of $\Delta E_{n,P'}(T)$ and delaying the rise of $C_{n,P'}(T)$. As T grows further, excitation to the 2 q.p. states starts contributing to $\langle\hat{H}\rangle_0$, and also to $\langle\hat{H}\rangle_{P'}$. If more and more q.p.'s are excited, the q.p. number distributes broadly, and the lack of the odd number-parity states is no longer important. Then $\Delta E_{n,P'}$ becomes vanishing again, and $C_{n,P'}$ also approaches

$C_{n,0}$. This feature is inherited in the number-projected result. Thus the occurrence of the S -shape in $C(T)$ is accounted for as effects of the number (or number-parity) conservation on the q.p. excitations.

In ^{161}Dy , the proton degrees-of-freedom are almost the same as in ^{162}Dy . $C_n(T)$, $\Delta E_n(T)$ and $\langle \hat{\mathcal{N}}_n \rangle$ in ^{161}Dy are presented in Fig. 3. In the graph of $C_n(T)$, we find an S -shape somewhat similar to that in ^{162}Dy , as a result of the projection. However, the S -shape in the projected result is less conspicuous, particularly around $T = T_c (\approx 0.6 \text{ MeV})$. It is remarked that similar even-odd difference is observed in the experiments [6] and in more realistic calculations [3, 5]. Moreover, we view small but non-vanishing values at low T ($0.05 \lesssim T \lesssim 0.2 \text{ MeV}$) in the projected results (see inset to Fig. 3(a)). These even-odd differences are again accounted for in terms of the q.p. excitation picture. Since the neutron number is odd in ^{161}Dy , the q.p. number should be 1 at $T \approx 0$, which is not taken into account in the unprojected result. Therefore, ΔE_n is higher by about $\Delta_n (\approx 1 \text{ MeV})$ at $T \approx 0$ than in ^{162}Dy . As T goes up, $\Delta E_{n,P'}$ decreases, because excitation to the 2 q.p. states predominantly contributes to $\langle \hat{H} \rangle_0$, which is eliminated in $\langle \hat{H} \rangle_{P'}$. For $T \gtrsim 0.5 \text{ MeV}$, many q.p. states mix up and the lack of even number q.p. states becomes less important. This leads to $\Delta E_{n,P'} \approx 0$. However, since $\Delta E_{n,P'}(T = 0)$ is higher than in ^{162}Dy , $\Delta E_{n,P'} \approx 0$ at $T \gtrsim 0.5 \text{ MeV}$ implies that $\Delta E_{n,P'}$ does not go up to a great extent at $T \approx T_c$, making the upper bend in the S -shape of $C_{n,P'}(T)$ weak. Although $\Delta E_{n,P}$ shifts downward, the full number projection gives analogous behavior. The structure in $C_n(T)$ at low T is also connected to the q.p. excitation. While there is only a single 0 q.p. state present in the even systems, there are several 1 q.p. states having close energy to one another. Hence, excitation from the lowest-lying 1 q.p. state to the higher-lying 1 q.p. states is possible even at low T . Note that this effect is only the cases for the projected statistics. To illustrate this mechanism, the q.p. number corresponding to the three Nilsson s.p. levels adjacent to ε_F and that for the next nearest six levels (three higher and three lower levels) are separately depicted in the inset to Fig. 3(c). Although $\langle \hat{\mathcal{N}}_n \rangle_P$ or $\langle \hat{\mathcal{N}}_n \rangle_{P'}$ stays unity at $T \lesssim 0.3 \text{ MeV}$, we view that excitation among the s.p. states occurs, giving small but non-negligible heat capacity.

As expected from the q.p. excitation picture, the above results are insensitive to nuclide, except that $C(T)$ at low $T (\lesssim 0.3 \text{ MeV})$ for odd nuclei somewhat depends on the s.p. levels around ε_F . This has been confirmed by calculations for neighboring Dy isotopes [15]. The q.p. excitation mechanism is so generic that it should not depend on the nuclear shapes, which has also been confirmed by calculations for Sn isotopes [15].

The number (or number-parity) conservation thus gives rise to the S -shapes in the heat capacity and their even-odd differences. Since it is explained within the q.p. excitation picture, the S -shaped heat capacity does not seem straightforwardly linked to the superfluid-to-normal transition. To investigate this point further, we try the following calculation: instead of solving the FT-BCS equation at each T , we keep using the solution at $T = 0$ for $\tilde{\varepsilon}_k$ and Δ_τ , and therefore for u_k and v_k . By this treatment the nucleus stays in the superfluid

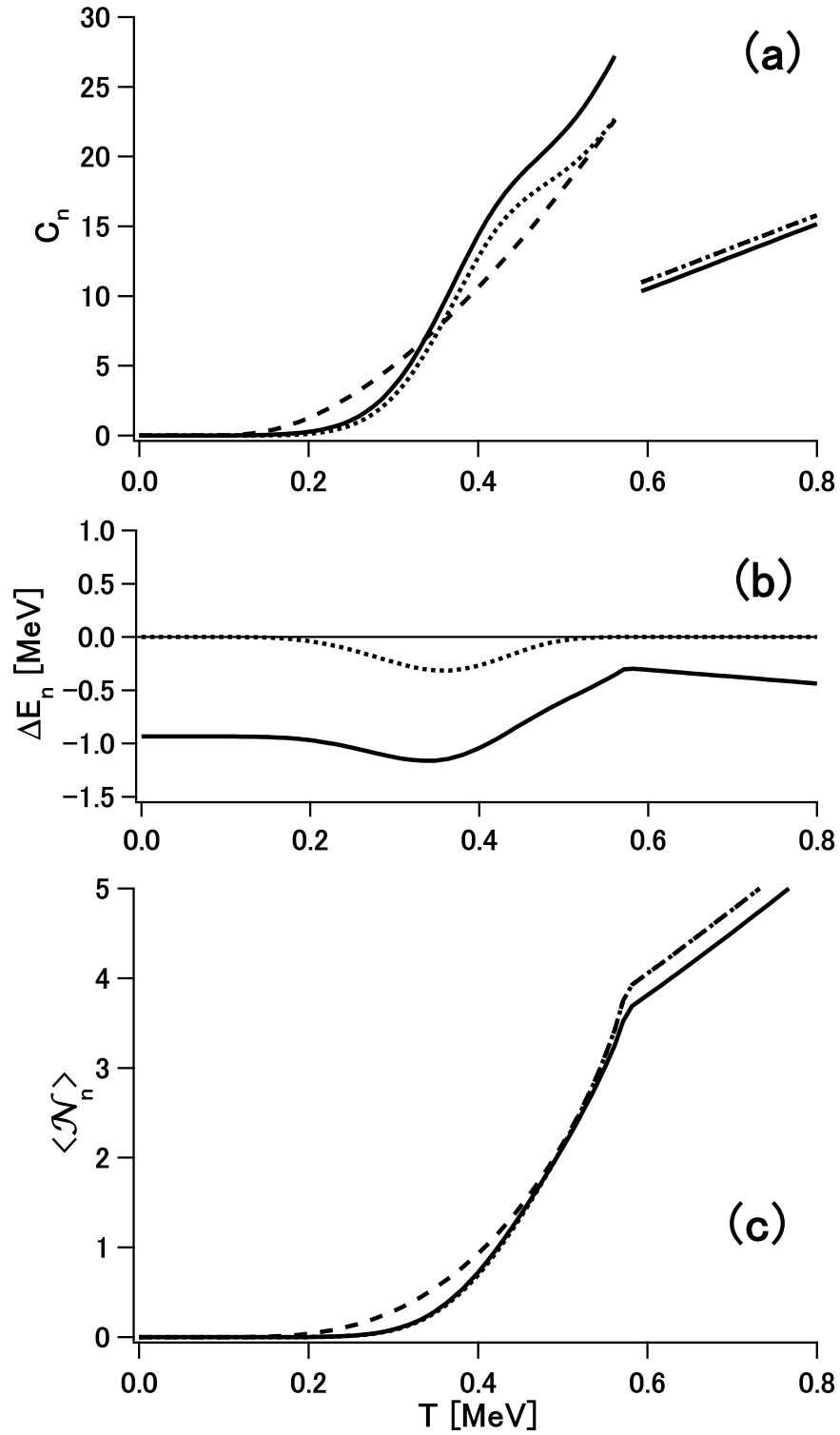


FIG. 2: Thermal properties of the neutron part of ^{162}Dy : (a) C_n , (b) ΔE_n , (c) $\langle \hat{\mathcal{N}}_n \rangle$, as functions of the temperature. See Fig. 1 for conventions.

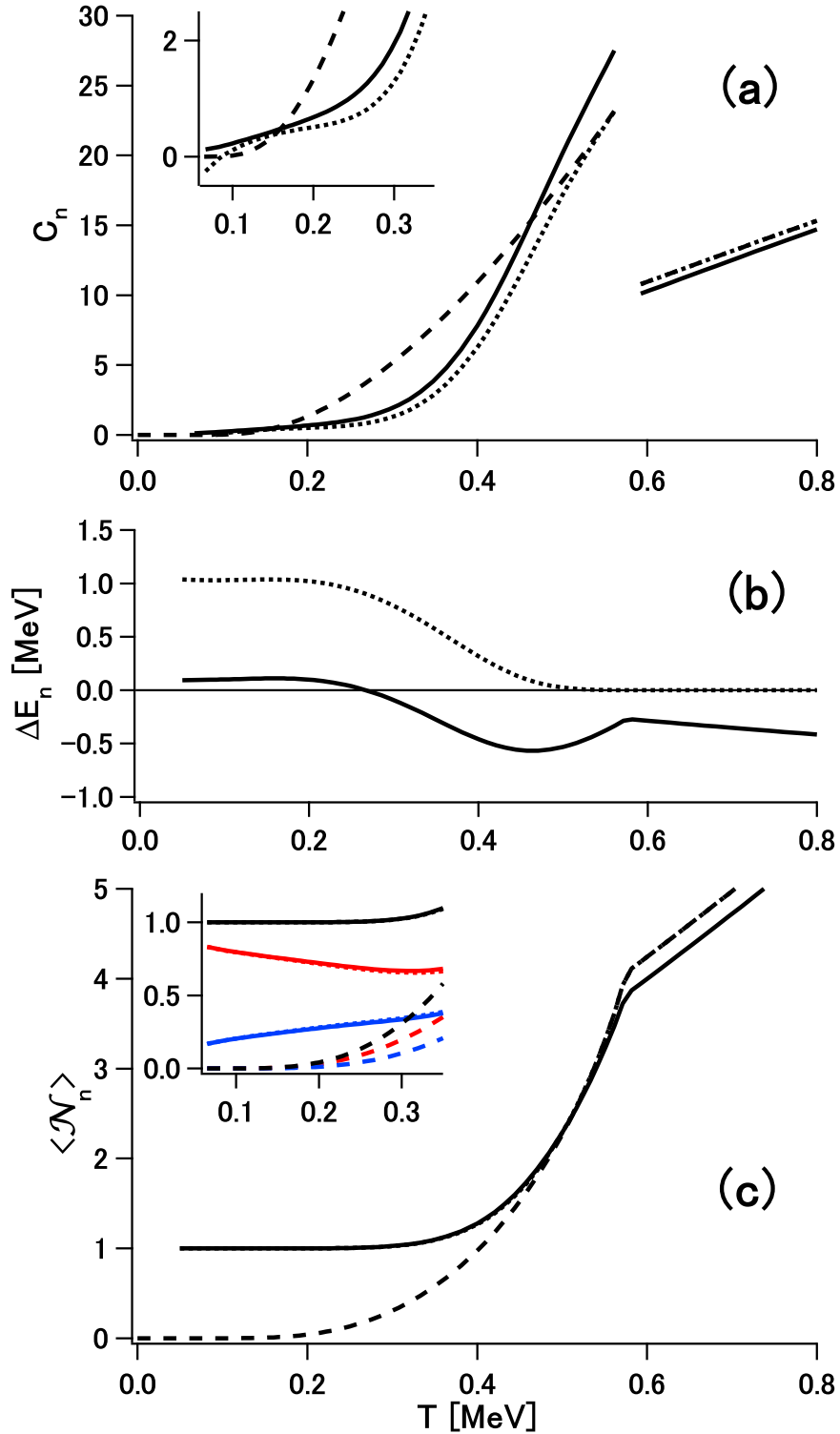


FIG. 3: Thermal properties of the neutron part of ^{161}Dy : (a) C_n , (b) ΔE_n , (c) $\langle \hat{\mathcal{N}}_n \rangle$. C_n at $0.07 < T < 0.35$ MeV is amplified in the inset to (a). In the inset to (c), $\langle \sum_{k \in \text{SP1}_n} \alpha_k^\dagger \alpha_k \rangle$ (red lines) and $\langle \sum_{k \in \text{SP2}_n} \alpha_k^\dagger \alpha_k \rangle$ (blue lines) are also presented as well as the total q.p. number (black lines), where SP1_n is composed of the Nilsson s.p. level with ε_F and the neighboring two (one higher and one lower) levels, while SP2_n consists of the next neighboring six (three higher and three lower) levels. See Fig. 1 for other conventions.

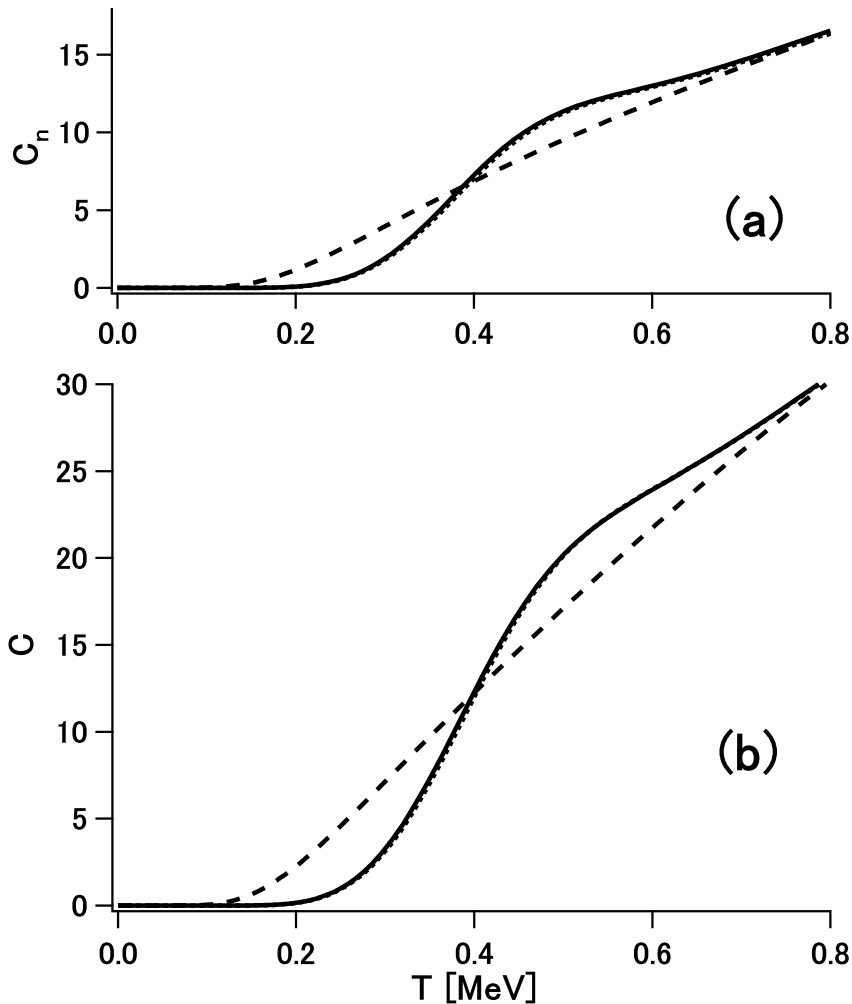


FIG. 4: Heat capacities for ^{162}Dy : (a) C_n and (b) C , with $\tilde{\epsilon}_k$ and Δ_τ fixed to be the $T = 0$ values.

phase at any T . The T -dependence enters only via the explicit one in the Boltzmann-Gibbs operator. Resultant C_n and $C = C_p + C_n$ are shown in Fig. 4 for ^{162}Dy , and in Fig. 5 for ^{161}Dy . We have the S -shapes even though the superfluidity is kept at any T . The even-odd differences in C are also viewed in this artificial model.

The observed S -shapes in $C(T)$ are deduced from the energy-dependence of the level densities [6]. We have confirmed that the present calculations with projection are qualitatively consistent with the measured level densities, whether or not \hat{H}_0 is T -dependent. However, the present results indicate a mechanism of the S -shapes in $C(T)$ different from the picture assumed in Ref. [6], in which the S -shapes emerge via continuity between the two phases. Still, one should not immediately conclude that the S -shapes shown in the present work are irrelevant to the transition. The T_c value in the present FT-BCS calculations is close to the temperature region where the S -shapes appear, as in the experiments, which may suggest

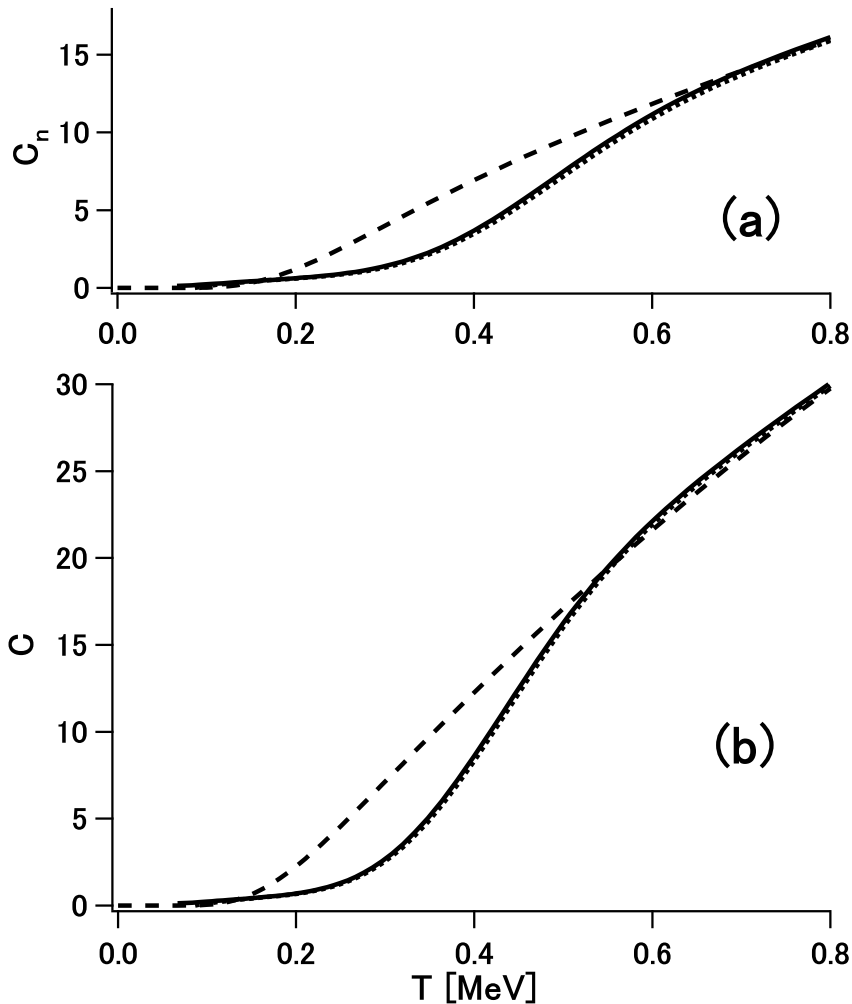


FIG. 5: Heat capacities for ^{161}Dy : (a) C_n and (b) C , with $\tilde{\varepsilon}_k$ and Δ_τ fixed to be the $T = 0$ values.

that the S -shapes might have correlation to the transition, even though their connection is not straightforward. For instance, suppose that the mixing of many q.p. states, which causes the upper bend of the S -shape in $C(T)$, also drives the phase transition in the BCS approximation, the S -shapes are indirectly correlated to the transition. It has been shown that the S -shapes take place (and the discontinuity at critical temperature is washed out) in realistic calculations [3, 5], in which various correlations are taken into account. However, in practice, relation of the S -shapes in $C(T)$ to the superfluid-to-normal phase transition has not yet been clear enough. It is desired to inspect carefully how individual quantum fluctuations affect the heat capacities of nuclei. We just point out here that the number conservation should play a certain role in producing the S -shapes, even though it may not be a full explanation. It is emphasized that effects of the conservation laws should not be discarded in discussing phase transitions in finite systems.

In summary, we have reexamined the heat-capacity of nuclei, applying the particle-number projection to the finite-temperature BCS theory. Since the projection is carried out after the variation, the sharp discontinuity at critical temperature remains which is not observed in experiments. While the S -shapes in the heat capacity have been claimed to be a fingerprint of the superfluid-to-normal phase transition, it is found that the particle-number projection gives S -shapes in the heat capacity of nuclei analogous to the observed ones, apart from the discontinuity. The even-odd difference in the heat capacity is also produced by the projection. Except low T part of odd nuclei, the number-parity projection gives similar heat capacity to the full number projection, if the s.p. energies are appropriately shifted. These S -shapes are accounted for in terms of the quasiparticle excitations, and occur even when we keep the superfluidity at all temperatures by assuming a constant gap in the BCS theory. Although the observed S -shapes could still correlate to the phase transition, their relation should be inspected carefully. The even-odd difference is also understood in the context of the quasiparticle excitations, in which the particle-number (or the number-parity) conservation plays a crucial role. The present study reveals significant role of the particle-number conservation in the heat capacity of nuclei.

The present work is financially supported as Grant-in-Aid for Scientific Research (B), No. 15340070, by the Ministry of Education, Culture, Sports, Science and Technology, Japan. Numerical calculations are performed on HITAC SR8000 at Information Initiative Center, Hokkaido University.

* Electronic address: nakada@faculty.chiba-u.jp

† Electronic address: tanabe@phy.saitama-u.ac.jp

- [1] S. Levit and Y. Alhassid, Nucl. Phys. **A413**, 439 (1984); H. Nakada and Y. Alhassid, Phys. Rev. Lett. **79**, 2939 (1997).
- [2] T. Døssing *et al.*, Phys. Rev. Lett. **75**, 1276 (1995).
- [3] R. Rossignoli, N. Canosa and P. Ring, Phys. Rev. Lett. **80**, 1853 (1998).
- [4] J. L. Egido, L. M. Robledo and V. Martin, Phys. Rev. Lett. **85**, 26 (2000).
- [5] S. Liu and Y. Alhassid, Phys. Rev. Lett. **87**, 022501 (2001).
- [6] A. Schiller *et al.*, Phys. Rev. C **63**, 021306(R) (2001); M. Guttormsen *et al.*, Phys. Rev. C **68**, 064306 (2003).
- [7] A. L. Goodman, Nucl. Phys. **A352**, 30 (1981).
- [8] K. Tanabe, K. Sugawara-Tanabe and H. J. Mang, Nucl. Phys. **A357**, 20 (1981).
- [9] K. Tanabe and H. Nakada, Phys. Rev. C **71**, 024314 (2005).
- [10] C. Esebbag and J. L. Egido, Nucl. Phys. **A552**, 205 (1993).
- [11] R. Rossignoli and P. Ring, Ann. Phys. (N.Y.) **235**, 350 (1994).
- [12] A. Bohr and B. R. Mottelson, *Nuclear Structure* vol. 2 (Benjamin, New York, 1975), Chap. 5.

- [13] S. Raman, C. W. Nestor Jr. and P. Tikkanen, *At. Data Nucl. Data Tables* **78**, 1 (2001).
- [14] M. Baranger and K. Kumar, *Nucl. Phys.* **A110**, 490 (1968).
- [15] K. Esashika, Master thesis, Chiba University, 2005 (unpublished, in Japanese).